

The *Arabidopsis* Nitrate Transporter NRT1.8 Functions in Nitrate Removal from the Xylem Sap and Mediates Cadmium Tolerance

Jian-Yong Li,^{a,1} Yan-Lei Fu,^{a,1} Sharon M. Pike,^b Juan Bao,^a Wang Tian,^c Yu Zhang,^a Chun-Zhu Chen,^a Yi Zhang,^a Hong-Mei Li,^a Jing Huang,^a Le-Gong Li,^c Julian I. Schroeder,^d Walter Gassmann,^b and Ji-Ming Gong^{a,2}

^aNational Key Laboratory of Plant Molecular Genetics, Institute of Plant Physiology and Ecology, Shanghai Institutes for Biological Sciences, Chinese Academy of Sciences, Shanghai 200032, People's Republic of China

^bDivision of Plant Sciences, C.S. Bond Life Sciences Center and Interdisciplinary Plant Group, University of Missouri, Columbia, Missouri 65211-7310

^cCollege of Life Sciences, Capital Normal University, Beijing 100037, People's Republic of China

^dDivision of Biological Sciences and Center for Molecular Genetics, Cell and Developmental Biology Section, University of California, San Diego, California 92093-0116

Long-distance transport of nitrate requires xylem loading and unloading, a successive process that determines nitrate distribution and subsequent assimilation efficiency. Here, we report the functional characterization of *NRT1.8*, a member of the nitrate transporter (*NRT1*) family in *Arabidopsis thaliana*. *NRT1.8* is upregulated by nitrate. Histochemical analysis using promoter- β -glucuronidase fusions, as well as in situ hybridization, showed that *NRT1.8* is expressed predominantly in xylem parenchyma cells within the vasculature. Transient expression of the *NRT1.8*:enhanced green fluorescent protein fusion in onion epidermal cells and *Arabidopsis* protoplasts indicated that *NRT1.8* is plasma membrane localized. Electrophysiological and nitrate uptake analyses using *Xenopus laevis* oocytes showed that *NRT1.8* mediates low-affinity nitrate uptake. Functional disruption of *NRT1.8* significantly increased the nitrate concentration in xylem sap. These data together suggest that *NRT1.8* functions to remove nitrate from xylem vessels. Interestingly, *NRT1.8* was the only nitrate assimilatory pathway gene that was strongly upregulated by cadmium (Cd^{2+}) stress in roots, and the *nrt1.8-1* mutant showed a nitrate-dependent Cd^{2+} -sensitive phenotype. Further analyses showed that Cd^{2+} stress increases the proportion of nitrate allocated to wild-type roots compared with the *nrt1.8-1* mutant. These data suggest that *NRT1.8*-regulated nitrate distribution plays an important role in Cd^{2+} tolerance.

INTRODUCTION

The nitrate assimilation pathway has been extensively studied. It consists of several steps, beginning with uptake into roots. Nitrate concentrations in soil vary considerably, mainly as a result of two microbial processes, mineralization and nitrification, that are highly sensitive to environmental conditions (Marschner, 1995). To cope with highly variable nitrate concentrations in soil, plants have developed both a high-affinity transport system (HATS) and a low-affinity transport system (LATS) (Glass et al., 1992; Crawford, 1995; Crawford and Glass, 1998; Forde, 2000). When the external nitrate concentration is high (>1 mM), LATS is preferentially used. When nitrate availability is limited, HATS is

activated and takes over the nitrate uptake process (Glass et al., 1992; Crawford and Glass, 1998).

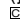
To date, two nitrate transporter gene families, *NRT1* and *NRT2*, were identified as responsible for LATS and HATS, respectively (Glass et al., 1992; Orsel et al., 2002b; Tsay et al., 2007). In the *Arabidopsis thaliana* *NRT1* family, the 53 *NRT1* (PTR, peptide transporter) members include both nitrate and oligopeptide transporters. Among the characterized nitrate transporters, CHLorate resistant 1 (CHL1/*NRT1.1*) is the most studied and represents a major low-affinity uptake mechanism for nitrate (Tsay et al., 1993, 2007). Furthermore, CHL1/*NRT1.1* functions as a dual-affinity transporter with regulation by phosphorylation (Wang et al., 1998; Liu et al., 1999). The *NRT2* family consists of seven members in the *Arabidopsis* genome. *NRT2.1* and *NRT2.2* are involved in inducible high-affinity nitrate uptake (Cerezo et al., 2001; Li et al., 2007). Though functionally and phylogenetically distinct, the nitrate transport functions of both *NRT1* and *NRT2* are believed to be proton dependent (Paulsen and Skurray, 1994; Orsel et al., 2002a).

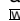
Once taken up into the root cytoplasm, nitrate is either translocated across the tonoplast and stored in the vacuoles, or it is reduced to nitrite and then partitioned to plastids where it is further assimilated to organic nitrogen (Orsel et al., 2002a).

¹ These authors contributed equally to this work.

² Address correspondence to jmgong@sibs.ac.cn.

The author responsible for distribution of materials integral to the findings presented in this article in accordance with the policy described in the Instructions for Authors (www.plantcell.org) is: Ji-Ming Gong (jmgong@sibs.ac.cn).

 Some figures in this article are displayed in color online but in black and white in the print edition.

 Online version contains Web-only data.

www.plantcell.org/cgi/doi/10.1105/tpc.110.075242

Alternatively, nitrate can be loaded into xylem vessels and subsequently unloaded (moved from the xylem sap into xylem parenchyma cells) in plant aerial tissues where it undergoes processes similar to those in roots (Marschner et al., 1997). So far, both the low-affinity nitrate transporter *NRT2.7* and the chloride channel, *CLCa*, were identified as responsible for short-distance nitrate translocation into vacuoles (De Angeli et al., 2006; Chopin et al., 2007). For long-distance transport, recent studies found that *NRT1.5* represents a major mechanism for loading nitrate into xylem vessels (Lin et al., 2008) and *NRT1.7* for loading nitrate into the phloem (Fan et al., 2009).

For herbaceous species, most of the nitrate undergoes long-distance transport to leaves where its assimilation can be directly coupled to photosynthesis in chloroplasts (Smirnov and Stewart, 1985; Andrews, 1986). However, the proportion of nitrate distributed to and assimilated in roots and shoots can vary substantially depending on the ambient environment. Under high light conditions, leaf assimilation is more energy efficient than root assimilation. However, when light intensity is limited, nitrate assimilation competes with CO₂ fixation for photochemical energy and reductants; thus, leaf assimilation is disadvantageous (Smirnov and Stewart, 1985). Prevalent root assimilation has also been reported when external nitrate availability is limited (Beevers and Hageman, 1980). These observations indicate that nitrate distribution between roots and shoots is of physiological importance in response to changing environments, though the regulating mechanisms remain largely unidentified.

In this study, we report the identification and characterization of *Arabidopsis* *NRT1.8*, which belongs to the 53-member *NRT1* family (Crawford and Glass, 1998; Tsay et al., 2007). We show

that *NRT1.8* is an inducible low-affinity transporter for nitrate that is localized in the plasma membrane of xylem parenchyma cells. Our results suggest that *NRT1.8* functions in taking up nitrate into xylem parenchyma cells, thus removing nitrate from the xylem sap, and that *NRT1.8*-mediated nitrate distribution plays a role in plant tolerance to Cd²⁺ stress.

RESULTS

Isolation and Characterization of *NRT1.8*

The *NRT1* gene family contains 53 members, with nitrate transporters having been identified in several divergent subfamilies (Tsay et al., 2007). Microarray data indicated that the *At4g21680* gene in the *NRT1* family is regulated by nitrate (Wang et al., 2003, 2004), suggesting that it might encode a nitrate transporter. Thus, we assigned the name *NRT1.8* to the *At4g21680* gene (Figure 1A). A full-length cDNA of *NRT1.8* was cloned using high-fidelity RT-PCR based on EST information from the Munich Information Center for Protein Sequences (<http://mips.gsf.de/proj/plant/jsf/athal/searchjsp/index.jsp>). The sequence was further confirmed by a BLAST search against The Arabidopsis Information Resource database (TAIR; <http://www.Arabidopsis.org/Blast/index.jsp>). *NRT1.8* is predicted to contain four exons and three introns (see Supplemental Figure 1A online), encoding a transmembrane protein with 589 amino acids and the typical 12 transmembrane domains observed in all other *NRT1* family members. The deduced protein sequence of *NRT1.8* is similar to all identified *NRT1*-type nitrate transporters and showed 64%

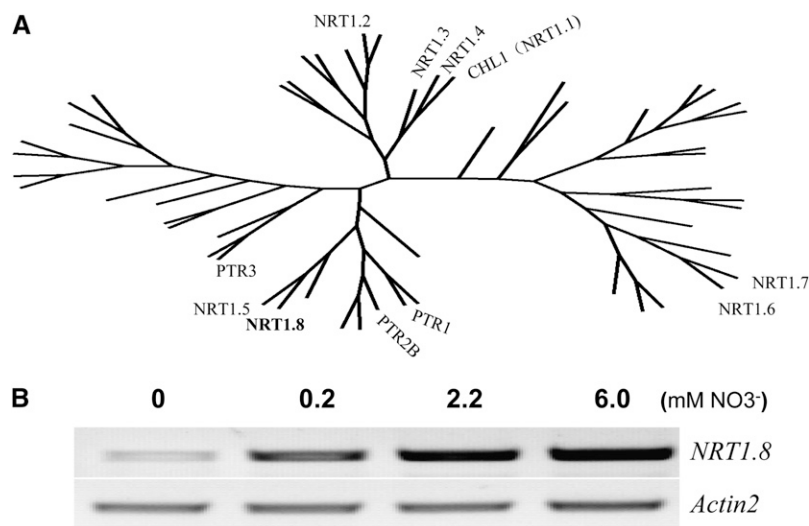


Figure 1. *NRT1.8* in the *Arabidopsis* *NRT1* Family Is Nitrate Responsive.

(A) Amino acid sequences of all 53 members in the *NRT1* family (Tsay et al., 2007) were downloaded from the TAIR website. Multiple alignment was performed using ClustalX 1.83 (Thompson et al., 1997) with default settings (protein gap open penalty, 10; protein gap extension penalty, 0.2; delay divergent sequences, 30%; use negative matrix, off; protein weight matrix, Gonnet series). The radial tree was drawn using PhyloDraw (Choi et al., 2000) based on the prior alignment result (see Supplemental Table 2 and Supplemental Data Set 1 online). Only characterized members are indicated.

(B) RT-PCR analysis of *NRT1.8* expression in roots under different external nitrate concentrations. The amplification cycles were 30 and 20 for *NRT1.8* and the loading control gene *Actin2*, respectively.

identity with NRT1.5 (Lin et al., 2008), its closest family member (Figure 1A).

We further performed RT-PCR to characterize the expression pattern of *NRT1.8* under various nitrate treatments. As shown in Figure 1B, after 3 d of nitrate starvation, a low level of *NRT1.8* mRNA was detected in roots. *NRT1.8* expression was induced by 0.2 mM NO₃⁻, and stronger induction was observed when 2.2 and 6 mM NO₃⁻ were added (Figure 1B). These results showed that *NRT1.8* is responsive to external nitrate in a concentration-dependent manner. In situ hybridization further confirmed this result (see Supplemental Figure 2 online).

***NRT1.8* Is Preferentially Expressed in *Arabidopsis* Vascular Tissues**

To determine the tissue-specific expression pattern of *NRT1.8*, histochemical analyses were performed using transgenic lines harboring the β-glucuronidase (*GUS*) gene driven by the *NRT1.8* promoter (*NRT1.8p:GUS*). As shown in Figure 2A, *GUS* activity was maximally and constitutively detected in the vasculature of *Arabidopsis* seedlings (Figure 2A). Cross-sectioned young seedling roots showed *NRT1.8p:GUS* expression within the stele

(Figure 2B). Longitudinal sectioning further demonstrated expression in parenchyma cells abutting xylem vessels (Figures 2C and 2D). These results suggested that *NRT1.8* may be involved in xylem loading or unloading.

We further performed mRNA in situ hybridization to exclude the possibility that *GUS* activity leakage was responsible for these results. Consistent with the *GUS* analysis, in situ hybridization also localized *NRT1.8* accumulation to xylem parenchyma cells in the stele (Figure 2E). In the control experiment using the sense *NRT1.8* probe, no signal was detected (Figure 2F). These results confirmed that the *GUS* activity analysis was reliable, and *NRT1.8* was expressed in xylem parenchyma cells within the vasculature.

Plasma Membrane Localization of NRT1.8

To investigate the subcellular localization of the *NRT1.8* protein, *NRT1.8* was fused in frame with enhanced green fluorescent protein (EGFP) and subcloned into the binary vector pGreenII. Transient expression of *NRT1.8:EGFP* in onion epidermal cells showed that green fluorescence was localized to the plasma membrane of plasmolyzed cells (Figures 3A and 3B) compared

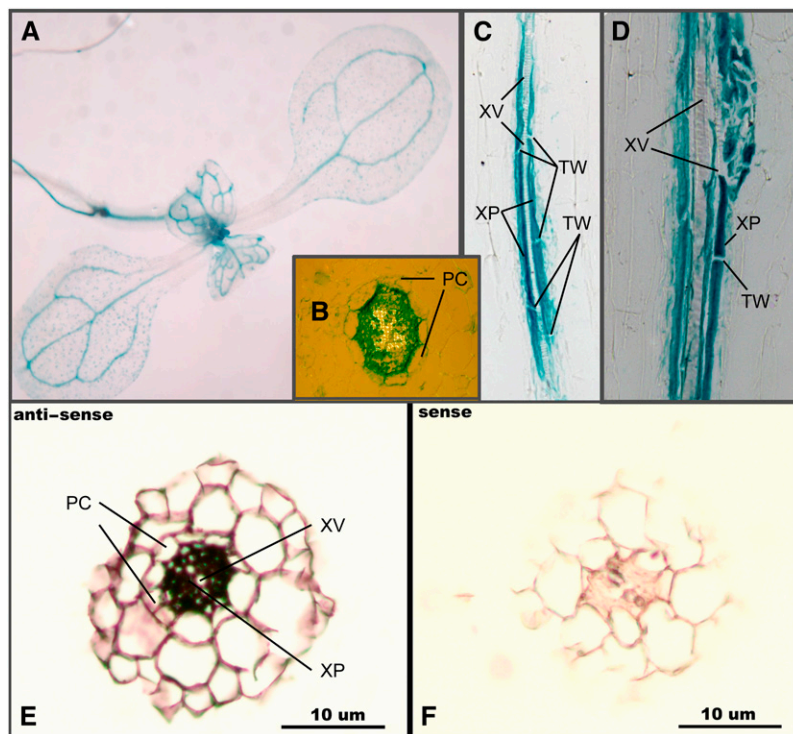


Figure 2. *NRT1.8* Is Expressed in Xylem Parenchyma Cells.

- (A) to (D) Histochemical localization of *GUS* activity in transgenic plants expressing the *GUS* reporter gene under the control of the *NRT1.8* promoter.
 - (A) Whole-mount seedlings.
 - (B) Cross-sectioned seedling roots.
 - (C) and (D) Longitudinally sectioned seedling roots.
 - (E) In situ hybridization of the antisense *NRT1.8* probe to a section of *Arabidopsis* root tissue.
 - (F) In situ hybridization of the sense *NRT1.8* probe to a section of *Arabidopsis* root tissue.
- PC, pericycle cells; XV, xylem vessels; XP, xylem parenchyma; TW, transverse cell wall.

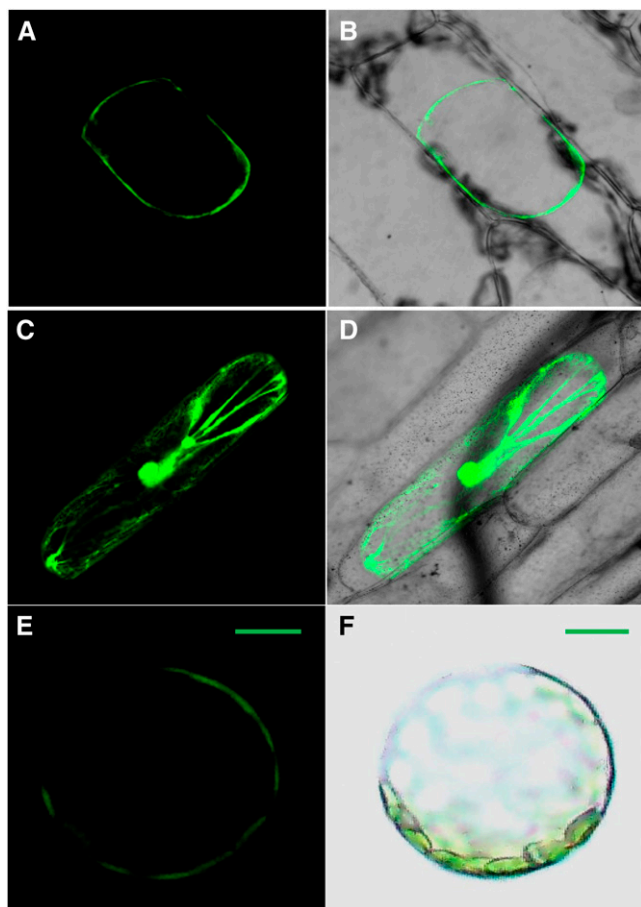


Figure 3. Subcellular Localization of NRT1.8.

Onion epidermal cells transiently transformed with either the NRT1.8:EGFP fusion or unfused EGFP were incubated in 0.8 M mannitol to induce plasmolysis and then imaged by confocal microscopy.

(A) Fluorescence image of epidermal cell expressing the NRT1.8:EGFP fusion protein.

(B) Merged EGFP fluorescence and bright-field image.

(C) Fluorescence image of epidermal cell expressing EGFP as a control.

(D) Merged control EGFP fluorescence and bright-field image.

(E) and (F) *Arabidopsis* protoplasts expressing the NRT1.8:EGFP protein (E) and bright-field image (F).

Bars = 20 μ M.

with the diffuse nucleocytoplasmic localization of the EGFP control (Figures 3C and 3D). To further confirm this result, we expressed NRT1.8:EGFP in *Arabidopsis* protoplasts. Consistently, green fluorescence was also observed at the protoplast plasma membrane (Figures 3E and 3F). These data indicated that NRT1.8 is plasma membrane localized.

NRT1.8 Can Transport Nitrate and Regulates Nitrate Removal from Xylem

Electrophysiological analyses were performed using *Xenopus laevis* oocytes injected with NRT1.8 cRNA to determine whether

NRT1.8 is a nitrate transporter. In uninjected oocytes, exposure to 10 mM nitrate at pH 5.5 induced a small inward current when oocytes were clamped to -40 mV (Figure 4A, top). On average, this current was approximately -20 nA (Figure 4B). By contrast, 11 out of 11 NRT1.8-injected oocytes from four separate batches

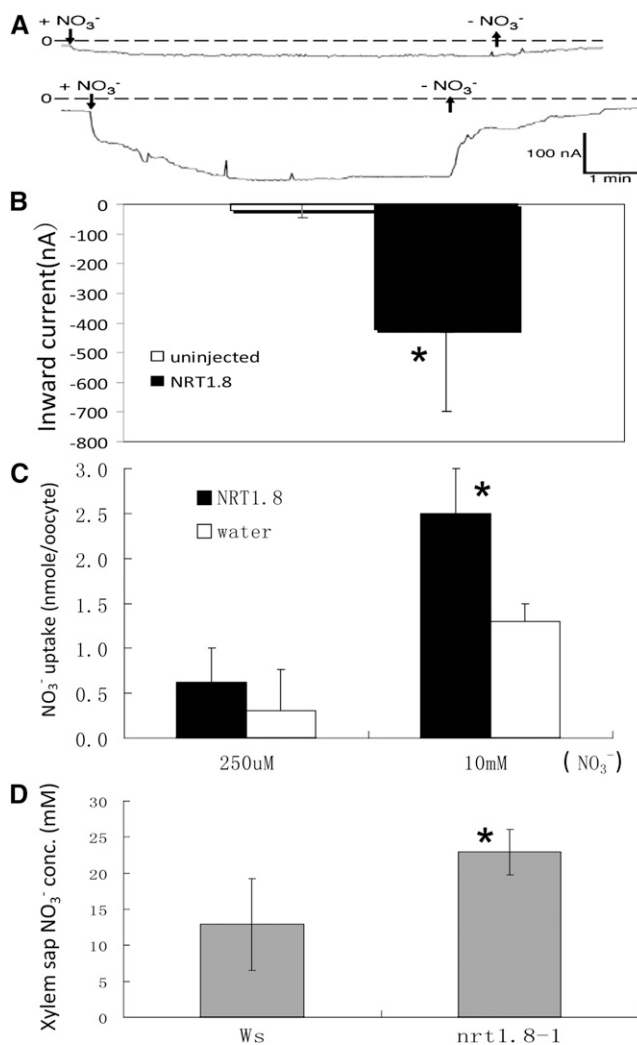


Figure 4. NRT1.8 Transports Nitrate.

(A) Representative inward currents elicited by 10 mM NO_3^- at pH 5.5 and a holding potential of -40 mV were recorded for control (top) and NRT1.8 cRNA injected oocytes (bottom).

(B) Quantification of the currents recorded; $*P < 0.001$, $n = 11$ for both injected and uninjected oocytes from four separate batches.

(C) High- and low-affinity nitrate uptake activity at pH 5.5. Oocytes were incubated for 3 h with 250 μ M or 10 mM nitrate. The amount of nitrate removed from the medium (high-affinity activity) or retained in the oocytes (low-affinity activity) was analyzed by HPLC as described by Huang et al. (1999). $*P < 0.01$, $n = 5$ samples for both high- and low-affinity uptake assays. Each sample consisted of four oocytes.

(D) NO_3^- concentration in xylem sap; $*P < 0.01$, $n = 6$ separate samples for both Ws and the *nrt1.8-1* mutant; each sample pooled sap from approximately nine independent plants. Error bars denote SD in (B) to (D).

showed large inward currents (Figure 4A, bottom), which averaged approximately -420 nA (Figure 4B). Uptake analyses in oocytes showed that NRT1.8 mediated nitrate uptake at 10 mM external nitrate, but not 250 μ M nitrate (Figure 4C), which is comparable to NRT1.5 (Tsay et al., 1993, 2007; Lin et al., 2008). To determine the apparent affinity of NRT1.8 for nitrate, we exposed oocytes to 1, 2, 5, and 10 mM HNO_3 at pH 5.5. In NRT1.8-injected oocytes, currents began to saturate at 10 mM nitrate (see Supplemental Figure 3 online). Higher nitrate concentrations induced leak currents also in uninjected control oocytes. Based on data from five oocytes from two batches, we calculated a K_m of NRT1.8 for nitrate of 12.0 ± 4.8 mM (error denotes SD). Currents at 10 mM nitrate averaged -340 ± 48 nA, whereas in uninjected oocytes, they averaged -38 ± 40 nA (average current from five oocytes from the same batches as NRT1.8-injected oocytes). We concluded that NRT1.8 is a low-affinity nitrate transporter.

In oocyte experiments, nitrate was added as HNO_3 . No additional monovalent mineral cations were present in the bath solution that contained 0.15 mM CaCl_2 (Huang et al., 1999). In addition, increasing external HNO_3 induced larger inward currents and shifted the reversal potential to more positive values. Together, these data indicated that the nitrate-induced inward current in NRT1.8-injected oocytes represents proton-coupled nitrate uptake. This is typical for most of the other characterized nitrate transporters in the NRT1 family (Tsay et al., 1993, 2007; Lin et al., 2008). Consistent with this, NRT1.8-mediated nitrate currents (Figure 5A) or uptake (Figure 5B) were larger than background at pH 5.5, but not at pH 7.4.

Considering that NRT1.8 is expressed in the plasma membranes of xylem parenchyma cells (Figures 2 and 3) and is a functional nitrate uptake transporter (Figures 4A to 4C), we suspected that NRT1.8 might function to take up nitrate into xylem parenchyma cells from the xylem. Disruption of NRT1.8 should thus result in nitrate accumulation in the xylem sap. To test this hypothesis, xylem sap was collected from wild-type Wassilewskija (Ws) plants and a T-DNA insertion mutant *nrt1.8-1*, in which full-length NRT1.8 transcript accumulation was not detected (see Supplemental Figure 1B online). As expected, the nitrate concentration in *nrt1.8-1* xylem sap was significantly higher than in that from Ws plants (Figure 4D, $P < 0.01$). These results suggest that NRT1.8 functions in transporting nitrate across xylem parenchyma cell membrane to unload nitrate from the xylem sap.

NRT1.8 Is Upregulated by Cd^{2+} Stress, and the *nrt1.8-1* Mutant Is Cd^{2+} Sensitive

NRT1.8 was initially identified based on its dramatic upregulation by Cd^{2+} stress in microarray experiments (see Supplemental Table 1 online) and hypothesized to provide an oligopeptide-mediated Cd^{2+} transport mechanism (Gong et al., 2003), since PTR-type oligopeptide transporters belong to the same family as NRT1 transporters (Tsay et al., 2007). However, our data demonstrate that NRT1.8 does not transport tripeptide glutathione (see Supplemental Figure 6 online) and is unlikely to transport the much larger oligopeptide phytochelatins (PCs/PCn, $n = 2$ to 11), the most studied Cd^{2+} chelators, but is a nitrate transporter

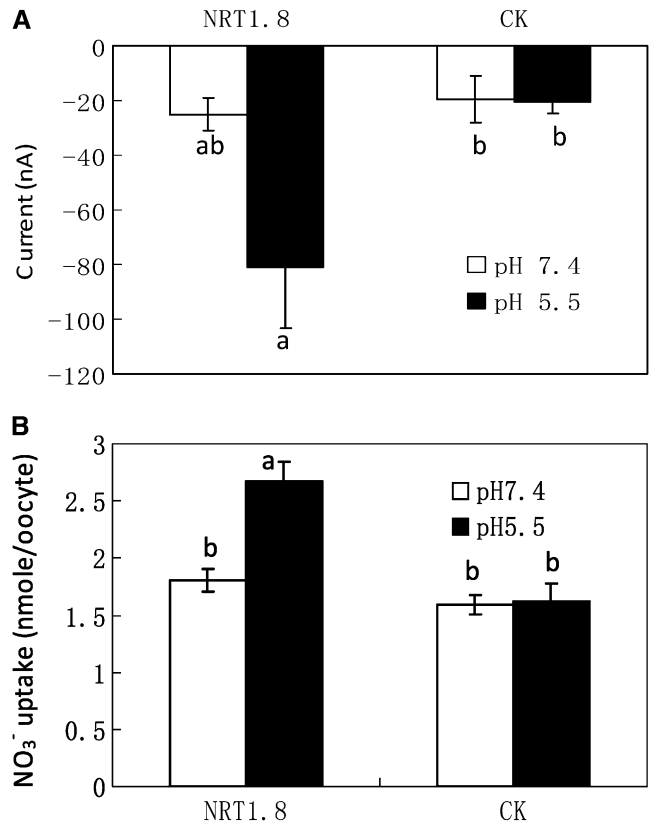


Figure 5. Nitrate Transport by NRT1.8 Is pH Dependent.

(A) Oocytes injected with NRT1.8 cRNA (NRT1.8) or uninjected oocytes (CK) were clamped at -20 mV and exposed to 5 mM HNO_3 at pH 7.4 (open bars) and subsequently at pH 5.5 (closed bars). Current differences before and after addition of 5 mM HNO_3 at each pH were averaged from four NRT1.8-injected and four uninjected oocytes from three batches. For NRT1.8, currents at pH 7.4 and 5.5 were statistically different at $P < 0.06$.

(B) Oocytes injected with NRT1.8 cRNA or uninjected oocytes were incubated with 10 mM nitrate for 3 h at pH 7.4 and 5.5, respectively. The amount of nitrate retained in oocytes was determined by HPLC. $n = 10$ samples from two batches, and each sample consisted of four oocytes. For NRT1.8, nitrate uptake at pH 5.5 and 7.4 was significantly different at $P < 0.001$.

Error bars denote SE. Lowercase letters indicate whether current averages were statistically different at $P < 0.05$ by t tests.

(Figure 4). Subsequently, we analyzed why Cd^{2+} strongly induces NRT1.8. The nonessential heavy metal Cd^{2+} has been observed to severely inhibit nitrate assimilation (Sanita di Toppi and Gabbriellini, 1999). Microarray analyses showed that NRT1.8 was the only gene in the nitrate assimilation pathway that was dramatically upregulated by Cd^{2+} stress (see Supplemental Table 1 online), suggesting that NRT1.8 might be an essential component in the interaction between nitrate assimilation and tolerance to Cd^{2+} stress.

To test our hypothesis, we performed RNA gel blots to confirm and further characterize the NRT1.8 expression pattern under Cd^{2+} stress. As shown in Figure 6A, NRT1.8 was undetectable in

roots without Cd^{2+} or with $40 \mu\text{M Cd}^{2+}$ for 6 h, while at 54 h, *NRT1.8* expression was significantly induced by $40 \mu\text{M Cd}^{2+}$. By contrast, $200 \mu\text{M Cd}^{2+}$ strongly induced *NRT1.8* within 6 h (Figure 6A). In shoots, in addition to a constitutively low expression, *NRT1.8* was also induced by long-term exposure to $40 \mu\text{M Cd}^{2+}$ (Figure 6B). Quantitative RT-PCR analyses further confirmed these results (Figure 6C). In roots, the *NRT1.8* mRNA level under the control condition was about 7% of that for the *Actin2* gene. When exposed to $20 \mu\text{M Cd}^{2+}$, the expression level gradually increased with prolonged exposure and reached ~13-fold of that for *Actin2* after 72 h (Figure 6C). Treatment with $200 \mu\text{M Cd}^{2+}$ rapidly and significantly induced *NRT1.8* expression in roots (Figure 6C; $P < 0.001$). By contrast, only prolonged Cd^{2+} treatment could significantly induce *NRT1.8* expression in shoots (Figure 6C, closed bars), most likely because of the time needed for Cd^{2+} transport and accumulation in shoots. These results indicated that Cd^{2+} regulates *NRT1.8* expression in a dose- and time-dependent manner, consistent with the expression pattern under NO_3^- induction (Figure 1B; see Supplemental Figure 2 online). Note that $200 \mu\text{M Cd}^{2+}$ is very toxic to plants; thus, long-term experiments were not performed at this Cd^{2+} concentration.

Subsequently, *in vivo* functional analyses were also performed. When grown on minimal medium supplemented with $50 \mu\text{M Cd}^{2+}$, both *nrt1.8-1* and Ws showed similar reduced growth (Figures 7B and 7E) compared with the control (Figures 7A and 7E). Considering that *NRT1.8* is a nitrate transporter, we then treated with various combinations of nitrate and Cd^{2+} . As shown in Figure 7C, when both 25 mM NO_3^- and $50 \mu\text{M Cd}^{2+}$ were applied, root elongation of *nrt1.8-1* was significantly reduced compared with

that of the wild type (Figures 7C and 7E; $P < 0.001$), while no significant difference was observed in rosettes (Figures 7B and 7C). When exposed to 25 mM NO_3^- only, no obvious difference was observed between *nrt1.8-1* and Ws (Figures 7D and 7E; $P > 0.19$). Further elevating NO_3^- to 50 mM (the nitrogen level in $1\times$ Murashige and Skoog medium is 60 mM) in combination with $50 \mu\text{M Cd}^{2+}$ resulted in a more apparent growth reduction in mutant aerial parts as well as secondary root formation (see Supplemental Figure 4C online). Complementation lines (see Supplemental Figure 1C online) harboring the genomic sequence of *NRT1.8* exhibited a less severe Cd^{2+} sensitivity phenotype comparable to the wild type (Figures 7A to 7D). These results indicated that the wild-type *NRT1.8* transporter increases Cd^{2+} tolerance in a nitrate-dependent manner in *Arabidopsis*.

Nitrate Distribution under Cd^{2+} Stress Is Altered by *NRT1.8*

To investigate the underlying mechanism of nitrate-dependent Cd^{2+} sensitivity, we determined the nitrate concentration in *Arabidopsis* shoots and roots, normalized by fresh weight to compare plant lines with differing growth rates. Under normal conditions, the nitrate level in both shoots and roots was similar in Ws, *nrt1.8-1*, and *NRT1.8/nrt1.8* plants. The root/shoot nitrate ratio was 0.38 in Ws, 0.37 in mutant *nrt1.8-1*, and 0.36 in the complementation line *NRT1.8/nrt1.8* (Figure 8A; $P > 0.55$). But when *NRT1.8* expression is strongly induced in roots by Cd^{2+} (Figures 6A and 6C), the proportion of nitrate concentration in Ws roots increased to 51% of that in shoots (a root/shoot nitrate ratio of 0.51; Figure 8B). By contrast, in the *nrt1.8-1* mutant, Cd^{2+} stress decreased the root/shoot nitrate ratio from 0.37 (Figure

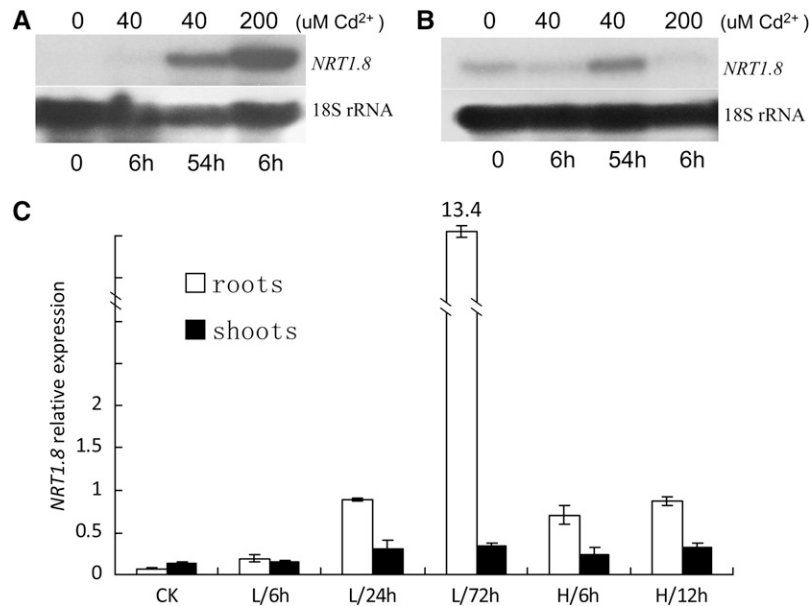


Figure 6. *NRT1.8* Expression under Cd^{2+} Stress.

(A) and (B) *NRT1.8* expression was determined in roots (A) and shoots (B) by RNA gel blotting after plants were exposed to 0, 40, and $200 \mu\text{M Cd}^{2+}$ treatment for the indicated times. 18S rRNA was used as a loading control.

(C) Quantitative RT-PCR analysis of *NRT1.8* expression in plants exposed to $20 \mu\text{M}$ (L) and $200 \mu\text{M}$ (H) Cd^{2+} for the indicated times. The y axis shows *NRT1.8* RNA levels normalized to that of *Actin2*. $n = 3$, and values are mean \pm SD. CK, control condition.

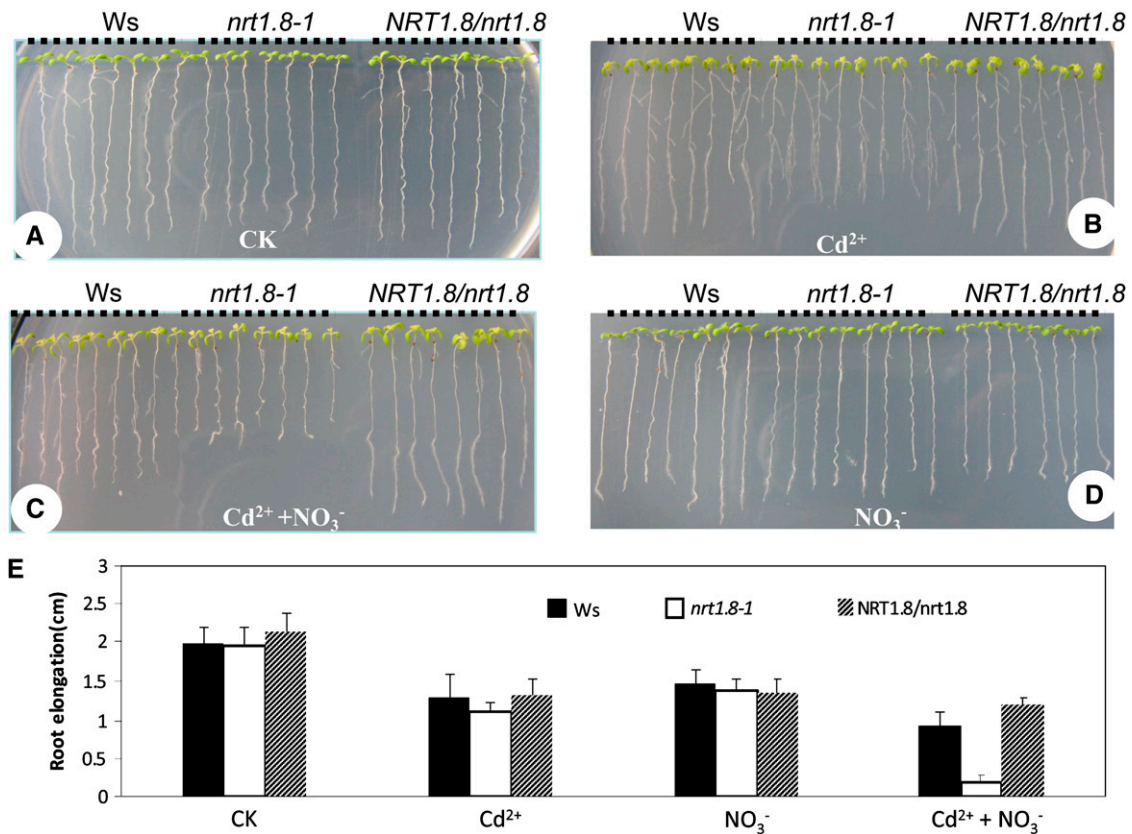


Figure 7. The *nrt1.8-1* Mutant is Cd²⁺ Sensitive.

(A) to (D) Plant growth under control condition (A), 50 M Cd²⁺ (B), 25 mM NO₃ plus 50 M Cd²⁺ (C), or 25 mM NO₃ (D). Black dotted lines indicate Ws, *nrt1.8-1*, and complementation line *NRT1.8/nrt1.8*, respectively. Images are not at same scale.

(E) Root elongation between days 2 and 10 after transfer to plates with treatments from (A) to (D). *n* = 7 to 8 plants, and values are mean ± SD. CK, control condition.

[See online article for color version of this figure.]

8A) to 0.32 (Figure 8B; *P* < 0.05). In the complementation lines, the Cd²⁺-induced root/shoot nitrate ratio alteration (an increase from 0.36 under control condition to 0.44 under Cd²⁺ stress) was comparable to that observed in the wild type. These data demonstrate that under Cd²⁺ stress, a greater proportion of nitrate accumulates in the wild-type Ws roots compared with *nrt1.8-1* (Figure 8B; *P* < 0.01) and suggest that the induction of *NRT1.8* in roots (Figures 6A and 6C) permits Ws to continue removing nitrate from the xylem when Cd²⁺ toxicity limits nitrate reductase activity. Note that under Cd²⁺ stress, the overall nitrate concentration was decreased in both Ws and *nrt1.8-1* mutant (Figures 8A and 8B), as would be expected due to Cd²⁺ toxicity (Hernandez et al., 1997; Sanita di Toppi and Gabbriellini, 1999).

The Cd²⁺ distribution within plants was also determined. As shown in Figure 9A, more Cd²⁺ accumulated in *nrt1.8-1* shoots when compared with both Ws and *NRT1.8/nrt1.8*, while in roots, less Cd²⁺ was detected in the mutant than in the wild type and the complementation lines (*P* < 0.05). Interestingly, more Cd²⁺ accumulation was also observed in xylem sap from *nrt1.8-1* than in sap from the wild-type control and the complementation lines (Figure 9B; *P* < 0.05).

***NRT1.5* and *NRT1.8* Expression Is Oppositely Regulated under Stresses**

NRT1.5 was shown to load nitrate into the xylem (Lin et al., 2008), and our data suggest that *NRT1.8* functions to unload nitrate from the xylem (Figures 2 to 4). Furthermore, our microarray data showed that *NRT1.5* and *NRT1.8* were oppositely regulated by Cd²⁺ stress (see Supplemental Table 1 online). These observations indicate that *NRT1.8* and *NRT1.5* may be fine-tuned to regulate nitrate distribution between shoots and roots under Cd²⁺ stress. To test our hypothesis, RNA gel blots were performed. As shown in Figure 10A, under control conditions, *NRT1.5* showed constitutively high expression in roots, while in shoots, no *NRT1.5* mRNA was detected. When treated with 200 μM Cd²⁺ for 6 h, *NRT1.5* expression was reduced (Figure 10A), as is observed in microarray analyses (see Supplemental Table 1 online). Further quantitative RT-PCR showed that in roots, low-level Cd²⁺ treatments (20 μM) gradually reduced *NRT1.5* mRNA levels with time, while high-level Cd²⁺ treatment rapidly and significantly reduced *NRT1.5* expression (Figure 10B, open bars). This was in contrast to what was observed for *NRT1.8* (Figure 6C,

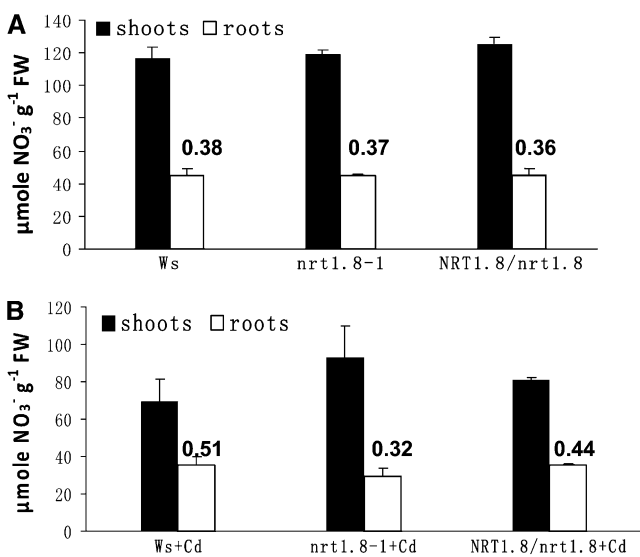


Figure 8. Nitrate Distribution Is Altered in the *nrt1.8-1* Mutant.

(A) NO_3^- concentration in wild-type (Ws), *nrt1.8-1* mutant, and *NRT1.8/nrt1.8* complementation plants under control conditions.

(B) NO_3^- concentration in wild-type (Ws), *nrt1.8-1* mutant, and *NRT1.8/nrt1.8* complementation plants under Cd^{2+} treatment.

The numbers above each bar represent the root/shoot nitrate ratio. Data were normalized to fresh weights (FW). Experiments were performed for six replicate samples, and each sample contained more than nine independent plants. Values are mean \pm SD.

open bars). In shoots, no significant change was observed for *NRT1.5* mRNA levels (Figure 10B, closed bars). Note that *NRT1.5* expression levels are very low in aerial parts (Figure 10A). Consequently, the standard deviation of *NRT1.5* expression levels in shoots measured by quantitative RT-PCR was large (Figure 10B, closed bars).

Further analyses revealed a similar opposite pattern between *NRT1.8* and *NRT1.5* mRNA level changes under various environmental stresses. As shown for some stress examples in Figure 10C, *NRT1.8* was consistently upregulated, while *NRT1.5* was downregulated, and more examples were found in the Genevestigator database (<https://www.genevestigator.com/gv/index.jsp>; Zimmermann et al., 2004). These observations suggest that the coordinated opposite regulation of *NRT1.5* and *NRT1.8* might be a universal mechanism in response to environmental stresses.

Lower Nitrate Accumulation in *nrt1.5* Xylem Sap

Considering that *NRT1.5* functions to load nitrate into the xylem, disruption of *NRT1.5* is expected to reduce the nitrate concentration in the xylem. A previous study observed that the rate of nitrate secretion into the xylem sap was reduced in *nrt1.5-1* (Lin et al., 2008). To complement our observation that the xylem sap nitrate concentration increased in the *nrt1.8-1* mutant (Figure 4D), we measured xylem sap nitrate concentrations in mutant lines of a different *NRT1* transporter, the allelic *NRT1.5* mutants

nrt1.5-3 and *nrt1.5-4*, in which intact *NRT1.5* mRNA was undetectable (Figures 11A and 11B). Consistent with our hypothesis that *NRT1.5* and *NRT1.8* have opposite functions, less nitrate accumulated in xylem sap of *nrt1.5* mutant plants compared with the wild-type control (Figure 11C), supporting that *NRT1.5* functions to load nitrate into the xylem (Lin et al., 2008).

DISCUSSION

Long-distance transport of nitrate determines nitrate distribution and subsequent assimilation between different tissues; thus, elucidation and regulation of the tightly controlled process would be of great importance to nutrient use efficiency (Marschner et al., 1997). In this study, we demonstrate that *NRT1.8*, a close homolog of *NRT1.5*, is a nitrate transporter and is expressed in xylem parenchyma cells. *nrt1.8-1* mutant plants show increased levels of nitrate in the xylem sap, consistent with the model that *NRT1.8* encodes a xylem unloading transporter.

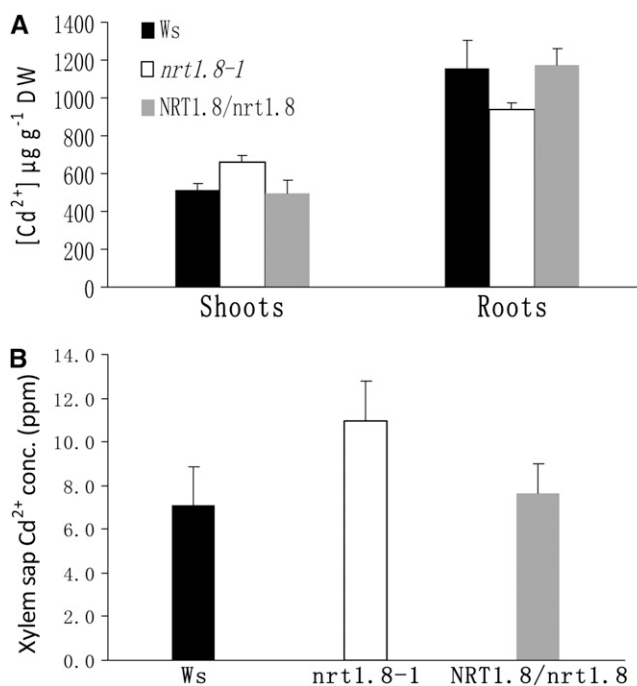


Figure 9. Cd^{2+} Distribution Is Altered in the *nrt1.8-1* Mutant.

(A) Cd^{2+} concentration in shoot and root tissues. Plants were grown hydroponically for 3 weeks and then exposed to 20 μM Cd^{2+} for 3 d. Shoots and roots were harvested and subjected to determination of Cd^{2+} concentration in the wild type (Ws), *nrt1.8-1* mutant, and complementation line *NRT1.8/nrt1.8*. Data were normalized to dry weight (DW). Experiments were performed for six replicates, and more than nine independent plants were pooled per replicate.

(B) Cd^{2+} concentration in xylem sap. Plants were treated with 5 μM Cd^{2+} for 3 d, xylem sap was collected as described in Methods, and Cd^{2+} concentration (conc.) was determined using inductively coupled plasma-mass spectrometry ($n = 6$).

Values are mean \pm SD.

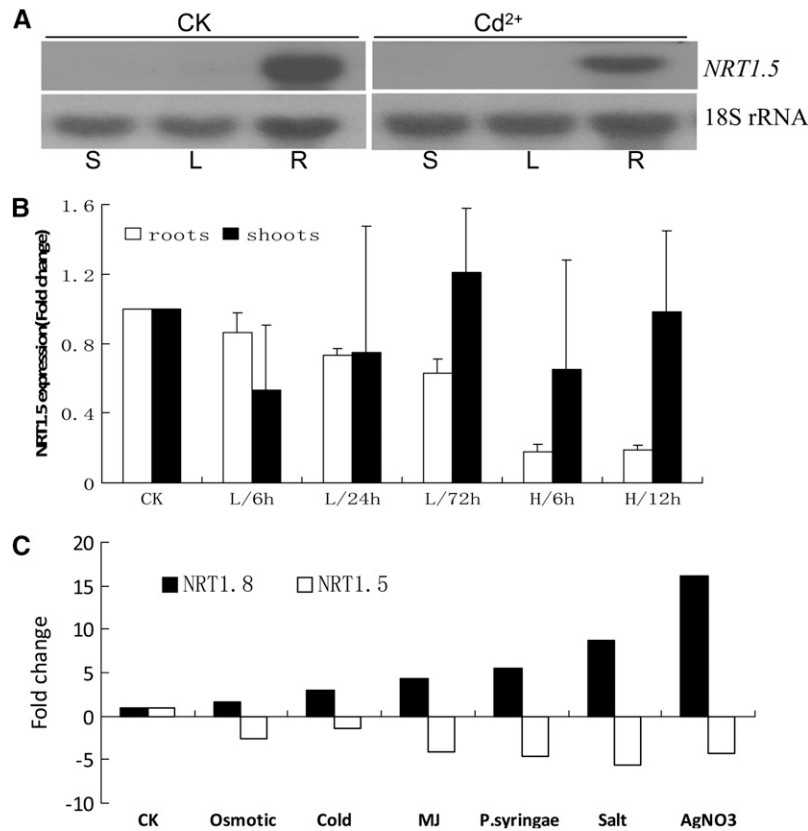


Figure 10. Opposite Regulation of *NRT1.8* and *NRT1.5* Expression under Stress Conditions.

(A) Four-week-old plants were exposed to 200 μM Cd^{2+} for 6 h or were kept under control conditions (CK). *NRT1.5* expression was determined in stems (S), rosette leaves (L), and roots (R) by RNA gel blots. 18S rRNA was used as a loading control.

(B) Quantitative RT-PCR of *NRT1.5* expression in plants treated with 20 μM (L) or 200 μM (H) Cd^{2+} for the indicated times. $n = 3$, and values are mean \pm SD. Fold change compared with control (CK) is shown.

(C) Expression data of *NRT1.8/At4g21680* and *NRT1.5/At1g32450* were obtained from Genevestigator (Zimmermann et al., 2004). Examples representing the following stresses were selected: osmotic (mannitol), cold (low temperature), MJ (methyl jasmonate), *P.syringae* (*Pseudomonas syringae*), salt (NaCl), and heavy metal (AgNO_3). Fold change compared with control (CK) is shown. Detailed information and more data are available from Genevestigator (<https://www.genevestigator.com/gv/index.jsp>).

NRT1.8 Functions to Remove Nitrate from Xylem Vessels

A transporter for nitrate loading into xylem sap was recently reported (Lin et al., 2008), and here we report a transporter for nitrate unloading from xylem sap. The *NRT1.8* gene from the NRT1 family was nitrate inducible (Figure 1B; see Supplemental Figure 2 online), which suggested that it might encode a low-affinity nitrate transporter. Electrophysiological analyses and nitrate uptake assays showed that *NRT1.8* mediates low-affinity nitrate uptake (Figures 4A to 4C). An inward current was elicited by millimolar nitrate in *NRT1.8* cRNA-injected oocytes at pH 5.5 (Figures 4A, 4B, and 5), consistent with a proton-coupled nitrate uptake model that is used by other identified *NRT1* family members (Tsay et al., 2007). Further analyses using GUS staining and in situ hybridization indicated that *NRT1.8* is expressed predominantly in the vasculature and located in xylem parenchyma cells (Figure 2), suggesting a functional role for *NRT1.8* in nitrate long-distance transport. Moreover, we show data dem-

onstrating that *NRT1.8* is localized to the plasma membrane (Figure 3) and that functional disruption of *NRT1.8* led to nitrate accumulation in xylem sap (Figure 4D). Taken together, we conclude that *NRT1.8* functions to remove nitrate from xylem vessels.

NRT1.8 Is an Essential Component Regulating Nitrate Distribution

Efficient long-distance transport of nitrate to aerial tissues of plants requires successive nitrate loading into the xylem and unloading to xylem parenchyma cells. Interestingly, consistent with the findings here that *NRT1.8* is a nitrate unloading transporter (Figure 4) and findings that *NRT1.5* is a nitrate loading transporter (Lin et al., 2008), an increased nitrate concentration was observed in *nrt1.8-1* xylem sap (Figure 4D), while *nrt1.5* mutants showed a decreased nitrate secretion rate into xylem

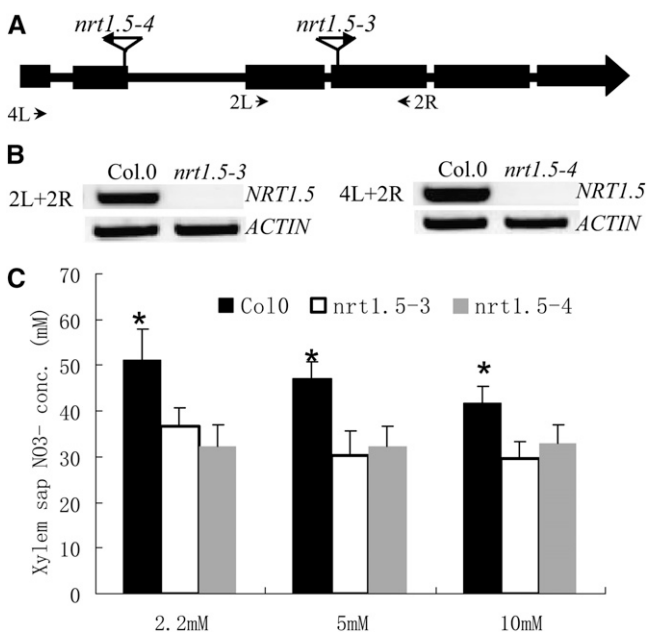


Figure 11. Decreased Nitrate Concentration in *nrt1.5* Xylem Sap.

(A) Schematic representation of two allelic T-DNA insertion lines *nrt1.5-3* (SAIL_72_F04) and *nrt1.5-4* (SALK_063393) were PCR screened and sequenced as described (Krysan et al., 1999) to identify homozygous mutants.

(B) RT-PCR did not detect intact *NRT1.5* mRNA in *nrt1.5-3* (left) and *nrt1.5-4* (right) mutant plants.

(C) The homozygous mutants and wild-type Columbia-0 were grown hydroponically for 4 weeks, subjected to nitrate starvation for 7 d, and then transferred to medium with 2.2, 5, or 10 mM nitrate for 12 h. Xylem sap was collected for 6 h, and nitrate concentrations were determined as described in Methods. Values are mean \pm SD, $n = 5$, and the asterisk indicates significant differences between wild-type Columbia-0 and the two mutant lines at $P < 0.01$.

(Lin et al., 2008) and reduced xylem sap nitrate concentrations (Figure 11C). Furthermore, *NRT1.8* and *NRT1.5* are closely related phylogenetically (Figure 1A). These data lead to the model that the distinct functions of *NRT1.8* and *NRT1.5* have evolved by subfunctionalization following an ancestral gene duplication event. Consistent with this postulation, when 4-week-old plants are under typical nonstress conditions, *NRT1.8* expression in shoots (Figure 6B) is higher than in roots (Figure 6A), and *NRT1.5* expression higher in roots than shoots (Figure 10A, CK). Under these conditions, *NRT1.5* and *NRT1.8* mainly effect the fine-tuning of long-distance nitrate transport from roots to shoots.

Subfunctionalization is also consistent with differential expression responses to environmental stresses. When under Cd²⁺ stress conditions, *NRT1.8* is upregulated while *NRT1.5* is down-regulated in *Arabidopsis* roots (see Supplemental Table 1 online; Figures 6A, 6C, 10A, and 10B). Similar expression patterns were observed repeatedly for *NRT1.8* and *NRT1.5* under various stress conditions, including salt, cold, metal stresses, and biotic stress (Figure 10C) (www.geneinvestigator.com/gv/index;

jsp; Zimmermann et al., 2004). These observations indicate that in addition to *NRT1.8*'s role in nitrate transport to aerial tissues, a more important role of *NRT1.8* might be to determine which tissues will accumulate nitrate in response to environmental cues. This hypothesis is supported by data showing that Cd²⁺ induces *NRT1.8* expression in roots (Figures 6A and 6C) with a corresponding increase in wild-type root nitrate concentration (Figures 8A and 8B). A similar mineral distribution mechanism has been reported for the xylem parenchyma cell-localized HKT1 (high-affinity K⁺ transporter 1) and SKC1 (Shoot K⁺ content 1) sodium transporters (Maser et al., 2002; Gong et al., 2004; Ren et al., 2005; Sunarpi et al., 2005). Disruption of these Na⁺ transporters results in overaccumulation of Na⁺ in xylem sap and shoots (Maser et al., 2002; Gong et al., 2004; Ren et al., 2005; Sunarpi et al., 2005; Horie et al., 2006; Davenport et al., 2007; Moller et al., 2009). Here, we observed that in the mutant *nrt1.8-1*, a greater proportion of nitrate accumulated in shoots under cadmium stress (Figure 8B). It is worth noting that *NRT1.8* expression is also induced in shoots under prolonged Cd²⁺ treatment (Figures 6B and 6C), which may contribute to recycling nitrate from shoots to roots. This would partially contribute to increasing the root/shoot nitrate ratio (Figure 8B), possibly via a similar mechanism proposed for HKT1/SKC1, in which Na⁺ is unloaded from xylem vessels to xylem parenchyma cells, then transported into the phloem and recycled to roots (Maser et al., 2002; Gong et al., 2004; Ren et al., 2005; Sunarpi et al., 2005; Horie et al., 2006; Davenport et al., 2007).

The Role of *NRT1.8*-Regulated Nitrate Distribution under Cadmium Stress

Cd²⁺, a nonessential toxic heavy metal, has long been observed to severely inhibit nitrate uptake, transport, and assimilation (Sanita di Toppi and Gabbriellini, 1999), resulting in biomass and protein content reduction (Chaffei et al., 2004). Furthermore, Cd²⁺ was also observed to affect nitrogen distribution in various plant species. In Cd²⁺-treated tomato (*Solanum lycopersicum*) seedlings, the total amino acid content increased in phloem and roots, together with an increase of glutamate dehydrogenase, cytosolic glutamine synthetase, and asparagine synthetase expression, suggesting that nitrogen was recycled and translocated from shoots to roots as a Cd²⁺ protection and storage strategy that may preserve roots (Chaffei et al., 2004).

In Cd²⁺-treated pea (*Pisum sativum*) plants, a similar NO₃⁻ distribution pattern was observed, and the authors proposed a model in which inhibited transpiration led to less nitrate transport to shoots and, thus, to nitrate accumulation in roots, resulting in a smaller decrease in root nitrate content under Cd²⁺ stress (Hernandez et al., 1997). Our data suggest that, in addition to this model of general reduction of transpiration-mediated nutrient translocation from roots to shoots, the *NRT1.8*-regulated nitrate accumulation in roots may represent a major mechanism in the process of nitrate distribution under Cd²⁺ stress, because the wild-type Ws maintained a higher root nitrate proportion than the *nrt1.8-1* mutant when plants were exposed to Cd²⁺ stress (Figure 8B). In addition, among all known nitrate assimilation pathway genes, only *NRT1.8* is dramatically upregulated in response to Cd²⁺ stress (see Supplemental Table 1 online; Figure

6). Thus, these data suggest that the alteration of the root/shoot nitrate ratio by NRT1.8 may represent an active regulatory process, rather than a passive consequence of inhibited transpiration.

Possible Interaction of Nitrate Distribution and Cd²⁺ Tolerance

Our findings raise the question of how nitrate distribution could affect Cd²⁺ tolerance. One possible explanation could be a mechanism similar to that observed for organic nitrogen redistribution, in which amino acids are transported from shoots to roots to preserve roots as nutritional safeguard organs, thus allowing future recovery (Chaffei et al., 2004). However, nitrate represents only a small proportion of all the nitrogen sources in roots, the direct nutritional effect of which might be subtle compared with that of organic nitrogen. Thus, a more plausible model is that NO₃⁻ serves as a signal molecule that enhances NR activity at elevated concentrations (Hernandez et al., 1995; Stitt, 1999). When recycled to roots, the proportionally increased nitrate induces NR and NiR activity otherwise inhibited by Cd²⁺, permitting nitrate uptake and assimilation to some extent. In *NRT1.8* overexpression lines, *CHL1*, nitrate reductase 1 (*NIA1*), nitrite reductase (*NIR*), and cytosolic glutamine synthase 1 (*GSR1*) were constitutively detected in roots and shoots under normal conditions (see Supplemental Figures 5C and 5D online). Interestingly, when exposed to Cd²⁺, lower reduction in *CHL1*, *NIA1*, *NIR*, and *GSR1* mRNA levels was observed in roots of *NRT1.8* overexpression lines compared with the wild type (see Supplemental Figures 5D and 5F online), as would be predicted by this model. The observation that Cd²⁺ sensitivity in *nrt1.8-1* is nitrate concentration dependent (Figure 7; see Supplemental Figure 4 online) and that a wild-type copy of *NRT1.8* rescues the phenotype further supports this hypothesis. Consistently, the *nrt1.5* mutant appears to exhibit increased tolerance to Cd²⁺ compared with the wild-type control (see Supplemental Figure 7 online).

Additionally, the Cd²⁺ allocation to shoots in *nrt1.8-1* plants may partially contribute to the Cd²⁺ sensitivity in the *nrt1.8-1* mutant (Figure 9). Cd²⁺ is highly toxic to plants, and most Cd²⁺ accumulates in roots to protect important organs (Gong et al., 2003). When *NRT1.8* was disrupted, more Cd²⁺ accumulated in mutant shoots than in wild-type shoots (Figure 9A), which thus would lead to greater Cd²⁺ toxicity in mutant plants. How nitrate distribution would affect Cd²⁺ allocation remains an open question. A previous study showed that in *Brassica juncea*, Cd²⁺ transport in the xylem sap was coordinated with nitrogen ligands (Salt et al., 1995). Additionally, nitrogen-containing molecules including phytochelatins and GSH have been detected concomitantly with Cd²⁺ transport in the vasculature (Gong et al., 2003; Chen et al., 2006; Li et al., 2006; Mendoza-Cozatl et al., 2008). Together, these data indicate that nitrate or nitrate-derived peptide and oligopeptide-assisted Cd²⁺ distribution may occur, permitting nitrogen-coordinated Cd²⁺ recycling and reduced Cd²⁺ accumulation in shoots in the wild type. However, it is worth noting that this process is not likely to be regulated by NRT1.8 directly, or at least not by NRT1.8-mediated transport of GSH or phytochelatins, the most studied Cd²⁺ chelators, be-

cause we could not obtain positive data showing that NRT1.8 could transport these chemicals (see Supplemental Figure 6 online).

In summary, *NRT1.8* encodes a nitrate transporter that mediates nitrate removal from the xylem sap, and functional characterization of the *NRT1.8* gene has revealed an important correlation between nitrate allocation and Cd²⁺ tolerance. Our research further indicates that nitrate allocation may be of essential importance for plant responses to environmental signals.

METHODS

Plant Materials, Growth Conditions, and Cd²⁺ Sensitivity Analyses

Arabidopsis thaliana plants were grown in quarter-strength sterile hydroponic solution at 22°C with 16-h-light/8-h-dark cycles as described (Arteca and Arteta, 2000; Gong et al., 2003). At 3 to ~4 weeks of age, plants were exposed to treatments as indicated. For Cd²⁺ sensitivity analyses, seedlings were grown for 7 d on quarter-strength Murashige and Skoog basal medium (Sigma-Aldrich) with 1 g/L MES, 0.8% (w/v) Suc, and 1.5% Bacto agar and then transferred to plates with basal medium or medium with either elevated nitrate levels or combinations of nitrate and 50 μM Cd²⁺ as indicated. Plants grew vertically for an additional 7 to 10 d, at which point root elongation was determined.

RNA Gel Blotting and RT-PCR/Quantitative RT-PCR

Four-week-old hydroponically grown plants were exposed to different level of Cd²⁺ stress for specified time intervals and other stresses as stated. Alternatively, plants were subjected to 3-d nitrate starvation, transferred to solutions with different levels of nitrate as indicated, and incubated for 2 h. Total RNA was extracted from roots and shoots using TRIzol reagent (Invitrogen) following the manufacturer's instructions and then separated in a formaldehyde/agarose gel and RNA gel blotting, probe labeling with isotope P³², and hybridization were performed according to standard protocols suggested by the manufacturers (GE Healthcare). X-ray film autoradiography was performed according to the manufacturer's protocol (Kodak) with an overnight exposure time to ensure linear detection of the indicated hybridization signals. First-strand cDNA was synthesized from DNaseI-digested total RNA using M-MLV reverse transcriptase (Promega), and PCR was performed on a PerkinElmer GeneAmp 9700 with indicated cycles (pilot experiments were performed to determine the optimal cycles for efficient and linear amplification of indicated genes) using Ex-Taq DNA polymerase (TaKaRa); PCR products were separated on 1% agarose gel and stained with ethidium bromide. Quantitative RT-PCR was performed on a Corbett Research Rotor-Gene 3000 thermal cycler using SYBR Premix Ex-Taq (TaKaRa) according to manufacturers' protocols; the primers used were as follows: *NRT1.8* (forward, 5'-GGCTTCAGATCTTGGATAG-3'; reverse, 5'-AACCACAGAGTAGAGGATGG-3'), *NRT1.5* (forward, 5'-TGT CATTGGACTTTCATCGC-3'; reverse, 5'-CCCACAACCTCTTGGTCTA ATC-3'). *Actin2* was used as an internal reference gene (forward, 5'-AGG TATCGTGTACCGTATGAG-3'; reverse, 5'-CATCTGCTGGAATGTGC TGA-3').

Histochemical Analysis and Tissue Sectioning

A 1309-bp genomic fragment immediately upstream from the *NRT1.8* start codon was amplified by PCR with forward primer (5'-TTAGATTGTT CGATTTCAGATTTAGG-3') and reverse primer (5'-AGGATCCCATAGATTC GATTTGGTGTAGAT-3'), which was then cloned into the vector

pGEM-T Easy (Promega), digested with *Hind*III and *Bam*HI, and subsequently cloned into binary expression vector pBI101-Hm2. The resulting construct pBHNRT was then transformed into Columbia-0 by the *Agrobacterium tumefaciens*-mediated floral dip method (Clough and Bent, 1998). GUS staining was performed for 16 h with 2 mM X-Gluc (5-bromo-4-chloro-3-indolyl- β -D-glucuronide), 5 mM $K_4Fe(CN)_6$, 5 mM $K_3Fe(CN)_6$, 0.2% Triton X-100, and 50 mM $NaPO_4$, pH 7.2 (68.4 parts of Na_2HPO_4 with 31.6 parts of NaH_2PO_4). The reaction was stopped by 70% ethanol. Tissue sectioning (8 μ m) was prepared for dark-field microscopy as described (Johnson et al., 2002).

In Situ Hybridization

One-week-old seedlings grown on quarter-strength Murashige and Skoog medium were transferred to nitrogen-depleted medium and grown for 3 d. They then were subjected to nitrate induction as indicated for 2 h. Tissue sectioning, digoxigenin labeling of RNA probe, and in situ hybridization were performed as described (Long and Barton, 1998) with minor modifications. A gene-specific fragment containing the 390-bp (983 to 1372) coding region of *NRT1.8* was amplified by PCR (forward, 5'-TGACTCAAGTCGAAGAAGTGAAG-3'; reverse, 5'-TTGAGATCGAAGTAGCACTTCC-3') and cloned into pGEM T Easy (Promega). Sense and antisense probes were in vitro synthesized using T7 and SP6 primers according to the manufacturer's instructions.

EGFP Fusion and Subcellular Localization

The stop codon of *NRT1.8* was mutagenized by PCR amplification to introduce a *Kpn*I site. This site was then used to make an in-frame *NRT1.8:EGFP* fusion construct. The final construct 35S/*NRT1.8:EGFP*-pGreenII and the empty vector 35S/*EGFP*-pGreenII were transiently expressed in onion epidermal cells using a particle gun-mediated system (PDS-1000/He; Bio-Rad). These constructs were also transiently expressed in *Arabidopsis* protoplasts via polyethylene glycol-mediated transformation (Yoo et al., 2007). The bombarded cells and transformed protoplasts were held in the dark at 22°C for 12 h followed by GFP imaging using confocal microscopy (Carl Zeiss; LSM 510 Meta) as described (Guo et al., 2003).

Functional Characterization of NRT1.8 in *Xenopus laevis* Oocytes

The *NRT1.8* cDNA was subcloned as a *Bam*HI-*Eco*RI fragment into the oocyte expression vector pOO2 (Ludewig et al., 2002), and cRNA was synthesized using the Ambion mMessage mMachine kit. *Xenopus* oocytes were isolated and maintained as described (Osawa et al., 2006) with the following modifications: oocytes were defolliculated for 30 to 90 min and were injected with 23 to 46 ng of *NRT1.8* cRNA on the same day or the day following isolation; oocytes were incubated in a ND-96 Ringer solution with antibiotics (96 mM NaCl, 2 mM KCl, 1 mM $MgCl_2$, 1.8 mM $CaCl_2$, 5 mM HEPES, 2.5 mM sodium pyruvate, 10 μ g/mL streptomycin sulfate, and 50 μ g/mL gentamycin sulfate, pH 7.4). Oocytes were voltage clamped 1 to 2 d after injection essentially as described (Osawa et al., 2006). Voltage clamp recordings were initiated in a bath solution containing 230 mM mannitol, 0.15 mM $CaCl_2$, and 10 mM MES/Tris, pH 5.5 (Huang et al., 1999). High- and low-affinity nitrate uptake assays were performed as described (Huang et al., 1999). Nitrate was added to the bath solution as HNO_3 at the indicated concentrations.

Isolation and Complementation of T-DNA Insertion Line

The *nrt1.8-1* mutant was isolated from the ALPHA T-DNA insertion population generated by the *Arabidopsis* Knockout Facility at the University of Wisconsin (Krysan et al., 1999). Primers used for PCR screening were *NRT1.8* forward primer (5'-AGTTAGACAGTTTGAGGTTTGCCTCAAG-3'), reverse primer (5'-GTAGAATCTCTCCAAGTGTCTTTG-

TTGA-3') and T-DNA left border primer JL202 (5'-CATTTTATAA-TAACGTGCGGACATCTAC-3'). RT-PCR was performed to verify knockout of the *NRT1.8* transcript using forward primer (5'-CTTTATCTACTGGTGCCTTATTGCT-3') and reverse primer (5'-ATAGAGATCAACTCTTCATGGTGC-3'). To make a complementation construct, a 2055-bp fragment containing the *NRT1.8* genomic sequence (–2 to 2053) was PCR amplified (forward, 5'-GGATCCATGGATCAAAAAGT-TAGACAGTT-3'; reverse, 5'-ATTTAGCTCCTGACTCAGACTTC-3'), sequenced, and subcloned into pBI101-Hm2 that was predigested with *Bam*HI and *Sac*I. The resulting construct was further digested with *Hind*III and *Bam*HI, into which the 1309-bp *NRT1.8* promoter fragment was inserted. The final construct containing both the *NRT1.8* promoter and coding regions was then used to transform the *nrt1.8-1* mutant as described above. Transgenic lines showing hygromycin resistance were selected and evaluated for Cd^{2+} sensitivity. The *nrt1.5* T-DNA insertion lines were ordered from the ABRC, and homozygous lines were screened and characterized by PCR as described (Krysan et al., 1999).

Determination of Nitrate and Cd^{2+} Levels

The *nrt1.8-1* mutant and its wild-type control Ws and complementation line *NRT1.8/nrt1.8* were grown in hydroponic solution for 4 weeks as described above and then transferred to hydroponic solution containing 10 mM nitrate or treatments as indicated for *nrt1.5* mutants and its wild-type Columbia-0. After 72 h incubation or as indicated, all rosette leaves were removed, the inflorescence stems were cut using a sharp razor, and xylem sap was collected for 6 h as described (Sunarpi et al., 2005). Alternatively, 3-week-old plants were exposed to 20 μ M Cd^{2+} when indicated and grown another 3 d before tissue harvest. To collect enough xylem sap for determination of Cd^{2+} concentrations, plants were instead exposed to a much less toxic Cd^{2+} treatment as indicated. Nitrate was extracted and determined by HPLC (Agilent 1200 series) using a PARTISIL 10 strong anion exchanger column (Whatman) as described (Chiu et al., 2004). Cd^{2+} was extracted and quantified using inductively coupled plasma-mass spectrometry as described (Gong et al., 2003) with minor modification.

Accession Numbers

Sequence data from this article can be found in the Arabidopsis Genome Initiative or GenBank/EMBL databases under the following accession numbers: CHL1 (At1g12110), *NRT1.2* (At1g69850), *NRT1.3* (At3g21670), *NRT1.4* (At2g26690), *NRT1.5* (At1g32450), *NRT1.6* (At1g27080), *NRT1.7* (At1g69870), *NRT1.8* (At4g21680), AT1G18880, AT1G22540, AT1G22550, AT1G22570, AT1G27040, AT1G33440, AT1G52190, AT1G59740, AT1G62200, AT1G68570, AT1G69860, AT1G72130, AT1G72140, AT2G02020, AT2G02040 (PTR2B), AT2G37900, AT2G38100, AT2G40460, AT3G01350, AT3G16180, AT3G25260, AT3G25280, AT3G43790, AT3G45650, AT3G45660, AT3G45680, AT3G45690, AT3G45700, AT3G45710, AT3G45720, AT3G47960, AT3G54140 (PTR1), AT5G01180, AT5G11570, AT5G13400, AT5G19640, AT5G28470, AT5G46040, AT5G46050 (PTR3), AT5G62680, AT5G62730, AT3G54450, AT1G72120, AT1G72125, AT3G53960, NIA1 (At1g77760), NIR (At2g15620), GSR1 (At5g37600), and Actin2 (At3g18780). All microarray data have been deposited in the National Center for Biotechnology Information/Gene Expression Omnibus database under the accession number GSE22114.

Supplemental Data

The following materials are available in the online version of this article.

Supplemental Figure 1. Isolation and Characterization of the T-DNA Insertion Line *nrt1.8-1* and Its Complementation Lines.

Supplemental Figure 2. *NRT1.8* Expression Was Upregulated in Response to External NO_3^- Concentration.

Supplemental Figure 3. NRT1.8 Is a Low-Affinity Nitrate Transporter.

Supplemental Figure 4. Cadmium Sensitivity in *nrt1.8-1* Was Increased with Higher Nitrate Level.

Supplemental Figure 5. Overexpression of *NRT1.8* Alters the Expression of Key Genes in the Nitrate Assimilation Pathway.

Supplemental Figure 6. Analysis of Substrate Selectivity for NRT1.8.

Supplemental Figure 7. *nrt1.5* Mutants Show Increased Tolerance to Cadmium Stress.

Supplemental Table 1. Transcriptomic Analysis of Nitrate Assimilation Pathway under Cd²⁺ Stress.

Supplemental Table 2. Accession Numbers of the Sequences Corresponding to Figure 1A.

Supplemental Data Set 1. Text File Corresponding to Figure 1A.

ACKNOWLEDGMENTS

We thank Minjung Kim and Daniel Schachtman (Donald Danforth Plant Science Center) for providing *NRT1.8* cloned into pO02 and *NRT1.8* cRNA, Xiao-Shu Gao (Core Facility, Shanghai Institute of Plant Physiology and Ecology, Shanghai Institutes for Biological Sciences) for helping with confocal microscopy, and the University of California, San Diego, GeneChip core and CapitalBio Co. for help with microarray experiments. This research was supported by the National Basic Research Program of China (2009CB119000), the National Science Foundation of China (30770179), the Chinese Academy of Sciences/State Administration of Foreign Experts Affairs International Partnership Program for Creative Research Teams and Chinese Academy of Sciences Innovation program (KSCX2-YW-N-056), and in part by the Shanghai Rising-Star Program (06QA14085) grants to J.-M.G. Initial *NRT1.8* experiments of J.-M.G. were supported by National Institute of Environmental Health Sciences (P42 ESI0337), Department of Energy (DOE-DE-FG02-03ER15449), and National Science Foundation (MCB-0918220) grants to J.I.S.

Received March 10, 2010; revised April 26, 2010; accepted May 10, 2010; published May 25, 2010.

REFERENCES

- Andrews, M.** (1986). The partitioning of nitrate assimilation between root and shoot of higher plants. *Plant Cell Environ.* **9**: 511–519.
- Arteca, R.N., and Arteca, J.M.** (2000). A novel method for growing *Arabidopsis thaliana* plants hydroponically. *Physiol. Plant.* **108**: 188–193.
- Beevers, L., and Hageman, R.** (1980). Nitrate and nitrite reduction. *The Biochemistry of Plants* **5**: 116–168.
- Cerezo, M., Tillard, P., Filleur, S., Munos, S., Daniel-Vedele, F., and Gojon, A.** (2001). Major alterations of the regulation of root NO₃⁻ uptake are associated with the mutation of *Nrt2.1* and *Nrt2.2* genes in *Arabidopsis*. *Plant Physiol.* **127**: 262–271.
- Chaffei, C., Pageau, K., Suzuki, A., Gouia, H., Ghorbel, M., and Masclaux-Daubresse, C.** (2004). Cadmium toxicity induced changes in nitrogen management in *Lycopersicon esculentum* leading to a metabolic safeguard through an amino acid storage strategy. *Plant Cell Physiol.* **45**: 1681–1693.
- Chen, A., Komives, E., and Schroeder, J.** (2006). An improved grafting technique for mature *Arabidopsis* plants demonstrates long-distance shoot-to-root transport of phytochelatin in *Arabidopsis*. *Plant Physiol.* **141**: 108–120.
- Chiu, C., Lin, C., Hsia, A., Su, R., Lin, H., and Tsay, Y.** (2004). Mutation of a nitrate transporter, *AtNRT1:4*, results in a reduced petiole nitrate content and altered leaf development. *Plant Cell Physiol.* **45**: 1139–1148.
- Choi, J.H., Jung, H.Y., Kim, H.S., and Cho, H.G.** (2000). PhyloDraw: A phylogenetic tree drawing system. *Bioinformatics* **16**: 1056–1058.
- Chopin, F., Orsel, M., Dorbe, M.-F., Chardon, F., Truong, H.-N., Miller, A.J., Krapp, A., and Daniel-Vedele, F.** (2007). The *Arabidopsis* *ATNRT2.7* nitrate transporter controls nitrate content in seeds. *Plant Cell* **19**: 1590–1602.
- Clough, S., and Bent, A.** (1998). Floral dip: A simplified method for *Agrobacterium*-mediated transformation of *Arabidopsis thaliana*. *Plant J.* **16**: 735–743.
- Crawford, N.** (1995). Nitrate: nutrient and signal for plant growth. *Plant Cell* **7**: 859–868.
- Crawford, N., and Glass, A.** (1998). Molecular and physiological aspects of nitrate uptake in plants. *Trends Plant Sci.* **3**: 389–395.
- Davenport, R., Muñoz-Mayor, A., Jha, D., Essah, P., Rus, A., and Tester, M.** (2007). The Na⁺ transporter *AtHKT1;1* controls retrieval of Na⁺ from the xylem in *Arabidopsis*. *Plant Cell Environ.* **30**: 497–507.
- De Angeli, A., Monachello, D., Ephritikhine, G., Frachisse, J.M., Thomine, S., Gambale, F., and Barbier-Brygoo, H.** (2006). The nitrate/proton antiporter *AtCLCa* mediates nitrate accumulation in plant vacuoles. *Nature* **442**: 939–942.
- Fan, S.-C., Lin, C.-S., Hsu, P.-K., Lin, S.-H., and Tsay, Y.-F.** (2009). The *Arabidopsis* nitrate transporter *NRT1.7*, expressed in phloem, is responsible for source-to-sink remobilization of nitrate. *Plant Cell* **21**: 2750–2761.
- Forde, B.G.** (2000). Nitrate transporters in plants: Structure, function and regulation. *Biochim. Biophys. Acta* **1465**: 219–235.
- Glass, A.D., Shaff, J., and Kochian, L.** (1992). Studies of the uptake of nitrate in barley: IV. Electrophysiology. *Plant Physiol.* **99**: 456–463.
- Gong, J., Lee, D., and Schroeder, J.** (2003). Long-distance root-to-shoot transport of phytochelatin and cadmium in *Arabidopsis*. *Proc. Natl. Acad. Sci. USA* **100**: 10118–10123.
- Gong, J., Waner, D., Horie, T., Li, S., Horie, R., Abid, K.B., and Schroeder, J.** (2004). Microarray-based rapid cloning of an ion accumulation deletion mutant in *Arabidopsis thaliana*. *Proc. Natl. Acad. Sci. USA* **101**: 15404–15409.
- Guo, F., Young, J., and Crawford, N.** (2003). The nitrate transporter *AtNRT1.1* (*CHL1*) functions in stomatal opening and contributes to drought susceptibility in *Arabidopsis*. *Plant Cell* **15**: 107–117.
- Hernandez, L., Garate, A., and Carpena-Ruiz, R.** (1997). Effects of cadmium on the uptake, distribution and assimilation of nitrate in *Pisum sativum*. *Plant Soil* **189**: 97–106.
- Hernandez, L., Ramon, A., Carpenarui, R., and Garate, A.** (1995). Evaluation of nitrate nutrition indexes in maize leaves - Metabolic nitrate, total nitrate content and nitrate reductase activity. *J. Plant Nutr.* **18**: 869–887.
- Horie, T., Horie, R., Chan, W.-Y., Leung, H.-Y., and Schroeder, J.I.** (2006). Calcium regulation of sodium hypersensitivities of *sos3* and *athkt1* mutants. *Plant Cell Physiol.* **47**: 622–633.
- Huang, N., Liu, K., Lo, H., and Tsay, Y.** (1999). Cloning and functional characterization of an *Arabidopsis* nitrate transporter gene that encodes a constitutive component of low-affinity uptake. *Plant Cell* **11**: 1381–1392.
- Johnson, C., Kolevski, B., and Smyth, D.** (2002). *TRANSPARENT TESTA GLABRA2*, a trichome and seed coat development gene of *Arabidopsis*, encodes a WRKY transcription factor. *Plant Cell* **14**: 1359–1375.
- Krysan, P., Young, J., and Sussman, M.** (1999). T-DNA as an insertional mutagen in *Arabidopsis*. *Plant Cell* **11**: 2283–2290.

- Li, W., Wang, Y., Okamoto, M., Crawford, N., Siddiqi, M., and Glass, A.** (2007). Dissection of the AtNRT2.1:AtNRT2.2 inducible high-affinity nitrate transporter gene cluster. *Plant Physiol.* **143**: 425–433.
- Li, Y., Dankher, O., Carreira, L., Smith, A., and Meagher, R.** (2006). The shoot-specific expression of $\{\gamma\}$ -glutamylcysteine synthetase directs the long-distance transport of thiol-peptides to roots conferring tolerance to mercury and arsenic. *Plant Physiol.* **141**: 288–298.
- Lin, S., Kuo, H., Canivenc, G., Lin, C., Lepetit, M., Hsu, P., Tillard, P., Lin, H., Wang, Y., Tsai, C., Gojon, A., and Tsay, Y.** (2008). Mutation of the *Arabidopsis* NRT1.5 nitrate transporter causes defective root-to-shoot nitrate transport. *Plant Cell* **20**: 2514–2528.
- Liu, K., Huang, C., and Tsay, Y.** (1999). CHL1 is a dual-affinity nitrate transporter of *Arabidopsis* involved in multiple phases of nitrate uptake. *Plant Cell* **11**: 865–874.
- Long, J., and Barton, M.** (1998). The development of apical embryonic pattern in *Arabidopsis*. *Development* **125**: 3027–3035.
- Ludwig, U., von Wiren, N., and Frommer, W.** (2002). Uniport of NH_4^+ by the root hair plasma membrane ammonium transporter LeAMT1;1. *J. Biol. Chem.* **277**: 13548–13555.
- Marschner, H.** (1995). *Mineral Nutrition of Higher Plants*, 2nd ed. (London: Academic Press), pp. 231–255.
- Marschner, H., Kirkby, E.A.B.C., and Engels, C.** (1997). Importance of cycling and recycling of mineral nutrients within plants for growth and development. *Bot. Acta* **110**: 265–273.
- Maser, P., et al.** (2002). Altered shoot/root Na^+ distribution and bifurcating salt sensitivity in *Arabidopsis* by genetic disruption of the Na^+ transporter AthKT1. *FEBS Lett.* **531**: 157–161.
- Mendoza-Cozatl, D., Butko, E., Springer, F., Torpey, J., Komives, E., Kehr, J., and Schroeder, J.** (2008). Identification of high levels of phytochelatin, glutathione and cadmium in the phloem sap of *Brassica napus*. A role for thiol-peptides in the long-distance transport of cadmium and the effect of cadmium on iron translocation. *Plant J.* **54**: 249–259.
- Moller, I.S., Gilliam, M., Jha, D., Mayo, G.M., Roy, S.J., Coates, J.C., Haseloff, J., and Tester, M.** (2009). Shoot Na^+ exclusion and increased salinity tolerance engineered by cell type-specific alteration of Na^+ transport in *Arabidopsis*. *Plant Cell* **21**: 2163–2178.
- Orsel, M., Filleur, S., Fraissier, V., and Daniel-Vedele, F.** (2002a). Nitrate transport in plants: Which gene and which control? *J. Exp. Bot.* **53**: 825–833.
- Orsel, M., Krapp, A., and Daniel-Vedele, F.** (2002b). Analysis of the NRT2 nitrate transporter family in *Arabidopsis*. Structure and gene expression. *Plant Physiol.* **129**: 886–896.
- Osawa, H., Stacey, G., and Gassmann, W.** (2006). ScOPT1 and AtOPT4 function as proton-coupled oligopeptide transporters with broad but distinct substrate specificities. *Biochem. J.* **393**: 267–275.
- Paulsen, I., and Skurray, R.** (1994). The POT family of transport proteins. *Trends Biochem. Sci.* **19**: 404.
- Ren, Z., Gao, J., Li, L.G., Cai, X., Huang, W., Chao, D., Zhu, M., Wang, Z., Luan, S., and Lin, H.X.** (2005). A rice quantitative trait locus for salt tolerance encodes a sodium transporter. *Nat. Genet.* **37**: 1141–1146.
- Salt, D., Prince, R., Pickering, I., and Raskin, I.** (1995). Mechanisms of cadmium mobility and accumulation in Indian mustard. *Plant Physiol.* **109**: 1427–1433.
- Sanita di Toppi, L., and Gabbriellini, R.** (1999). Response to cadmium in higher plants. *Environ. Exp. Bot.* **41**: 105–130.
- Smirnov, N., and Stewart, G.** (1985). Nitrate assimilation and translocation by higher plants: Comparative physiology and ecological consequences. *Physiol. Plant.* **64**: 133–140.
- Stitt, M.** (1999). Nitrate regulation of metabolism and growth. *Curr. Opin. Plant Biol.* **2**: 178–186.
- Sunarp, et al.** (2005). Enhanced salt tolerance mediated by AthKT1 transporter-induced Na^+ unloading from xylem vessels to xylem parenchyma cells. *Plant J.* **44**: 928–938.
- Thompson, J.D., Gibson, T.J., Plewniak, F., Jeanmougin, F., and Higgins, D.G.** (1997). The CLUSTAL_X windows interface: Flexible strategies for multiple sequence alignment aided by quality analysis tools. *Nucleic Acids Res.* **25**: 4876–4882.
- Tsay, Y.F., Chiu, C.C., Tsai, C.B., Ho, C.H., and Hsu, P.K.** (2007). Nitrate transporters and peptide transporters. *FEBS Lett.* **581**: 2290–2300.
- Tsay, Y.-F., Schroeder, J.I., Feldmann, K.A., and Crawford, N.M.** (1993). The herbicide sensitivity gene CHL1 of *Arabidopsis* encodes a nitrate-inducible nitrate transporter. *Cell* **72**: 705–713.
- Wang, R., Liu, D., and Crawford, N.** (1998). The *Arabidopsis* CHL1 protein plays a major role in high-affinity nitrate uptake. *Proc. Natl. Acad. Sci. USA* **95**: 15134–15139.
- Wang, R., Okamoto, M., Xing, X., and Crawford, N.M.** (2003). Microarray analysis of the nitrate response in *Arabidopsis* roots and shoots reveals over 1,000 rapidly responding genes and new linkages to glucose, trehalose-6-phosphate, iron, and sulfate metabolism. *Plant Physiol.* **132**: 556–567.
- Wang, R., Tischner, R., Gutierrez, R.A., Hoffman, M., Xing, X., Chen, M., Coruzzi, G., and Crawford, N.M.** (2004). Genomic analysis of the nitrate response using a nitrate reductase-null mutant of *Arabidopsis*. *Plant Physiol.* **136**: 2512–2522.
- Yoo, S., Cho, Y., and Sheen, J.** (2007). *Arabidopsis* mesophyll protoplasts: A versatile cell system for transient gene expression analysis. *Nat. Protoc.* **2**: 1565–1572.
- Zimmermann, P., Hirsch-Hoffmann, M., Hennig, L., and Gruissem, W.** (2004). GENEVESTIGATOR. *Arabidopsis* microarray database and analysis toolbox. *Plant Physiol.* **136**: 2621–2632.